PROCEEDINGS, TOUGH Symposium 2006
Lawrence Berkeley National Laboratory, Berkeley, California, May 15–17, 2006

GAS PRODUCTION BY DEPRESSURIZATION FROM HYPOTHETICAL CLASS 1G AND CLASS 1W HYDRATE RESERVOIRS

Doruk Alp[1]*, Mahmut Parlaktuna[1], George J. Moridis[2]

[1] Department of Petroleum and Natural Gas Engineering, Middle East Technical University
Ankara, 06531, Turkey
e-mail: doruk@psu.edu (* now with PSU)
e-mail: mahmut@metu.edu.tr

[2] Lawrence Berkeley National Laboratory, University of California
Berkeley, CA, 94720, USA
e-mail: gjmoridis@lbl.gov

ABSTRACT

A study on recovery of gas from a Class 1G hydrate deposit (mobile gas in the hydrate zone) and a Class 1W hydrate deposit (mobile water in the hydrate zone) is presented in this text. During the production from these reservoirs, a second dissociation front appears at the top of the hydrate interval. This front develops and advances downward in addition to the original hydrate interface. Two production schemes; with and without well-bore heating (case A and case B), show the same replenishment rate of produced hydrate under the conditions studied. For the case with well-bore heating and 20 years production life, hydrate dissociation contributes up to 50% of the production rate and up to 38% of the cumulative volume of produced gas. High-low alternating hydrate saturation layers (hydrate lens) are observed in both types of reservoirs for both cases of well-bore heating.

INTRODUCTION

Natural gas hydrates, which resemble ice, are clathrate compounds of water and hydrocarbon molecules, forming under proper temperature and pressure conditions.

Through a phase change and hydrogen bonding, several water molecules build a cage enclosing the hydrocarbon molecule (mostly methane, CH_4) and this cage structure is the foundation for crystalline nature of solid hydrate substance.

In this study, using equilibrium model of dissociation, it is aimed to model gas production by depressurization from a hypothetical Class 1 hydrate reservoir (Moridis & Collett, 2003). In a Class 1 hydrate reservoir only the upper part of reservoir is within the hydrate window and below this hydrate zone there is high saturation mobile gas. Hence, it is convenient to decompose the hydrate and produce the entrapped gas by relieving the exerted fluid pressure on hydrate through production of the initially free gas.
TOUGH-Fx/Hydrate (Moridis et al., 2005), the hydrate module for the new version of well known multipurpose thermal reservoir simulator TOUGH2 (Pruess et al., 1999), is utilized in order to carry out the non-isothermal analysis since hydrate equilibrium pressure is very sensitive to temperature change and decomposition of hydrate is a substantially endothermic process.

GOVERNING EQUATIONS

Hydrate formation pressure for temperatures above 0°C are computed using the equilibrium pressure equation (Moridis, 2002):

$$\begin{aligned}\ln(\mathrm{Pe}) = &-1.94138504464560 * 10^{5} + 3.31018213397926 * 10^{3} * \mathrm{T}\\ &- 2.25540264493806 * 10 * \mathrm{T}^{2} + 7.67559117787059 * 10^{-2} * \mathrm{T}^{3}\\ &- 1.30465829788791 * 10^{-4} * \mathrm{T}^{4} + 8.86065316687571 * 10^{-8} * \mathrm{T}^{5}\end{aligned}$$

Dissociation enthalpy of hydrate is estimated using Clapeyron equation (Sloan, 1990) and appended to the general energy equation which is solved simultaneously with mass balance equations:

$$\frac{d(\ln P)}{dT} = \frac{\Delta H}{znRT^2}$$

Thermal conductivity of a grid is calculated through the Equation which is derived by Moridis et al (2005):

$$k = k_{dry} + \left(\sqrt{S_A} + \sqrt{S_H}\right)\left(k_{wet} - k_{dry}\right) + \phi S_I \lambda_I$$

Change in permeability due to solid formation in pore space is accounted through “Original Porous Medium” (OPM) model available in TOUGH-Fx (Moridis et al., 2005).

This model does not provide a permeability reduction factor and in essence benefits from the fact that effective permeability to a phase (k_β) is a function of the phase saturation (S_β) and with increasing solid saturation there is an inevitable reduction in the saturation of mobile phase. Hence absolute permeability reduction is introduced within relative permeability changes:

$$k_{r\beta} = k_{r\beta}\left(S_{\beta}\right)$$
$$k_{\beta} = k_0 k_{r\beta}$$

Relative permeability changes are accommodated using Stone's model (Moridis et al., 2005) provided within TOUGH-Fx (Figure 1).

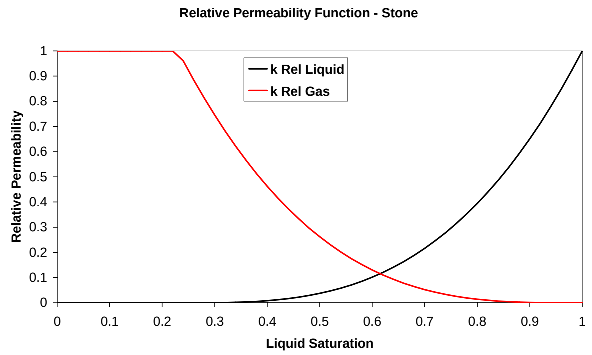

Figure 1: Relative permeability function - Stone

Capillary pressure is modeled using the van Genuchten function (Pruess et al., 1999) which is also embedded in TOUGH-Fx (Figure 2).

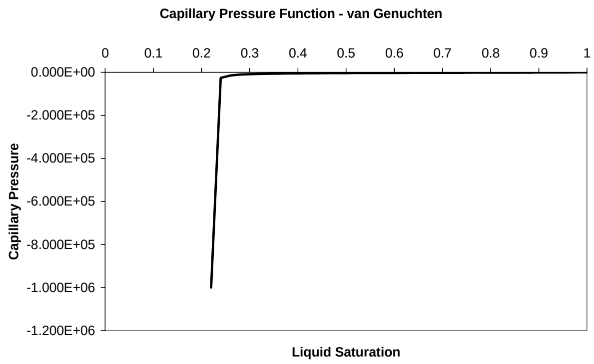

Figure 2: Capillary pressure function - van Genuchten

For the Class 1W reservoir, the need for using two distinct capillary pressure functions for the upper and lower sections has risen in order to retain the approximately ~30% liquid saturation (which is significantly above the irreducible saturation of ~25%) all along the upper and lower sections. This may be interpreted as two different porous mediums being defined in the reservoir.

While a van Genuchten type capillary pressure is suitable for lower section, to be able to sustain ~30% liquid saturation initially in the hydrate zone, a function which gives high capillary pressures even at high liquid saturations is required. Therefore; for the upper section of class 1W reservoir, a modified (continuous at S_l=1.0) Brooks - Corey function was defined in TOUGH-Fx/Hydrate (Moridis et al., 2005). With this equation (Figure 3) though the liquid in the hydrate zone is initially hold in place, it can be moved with adequate pressure difference.

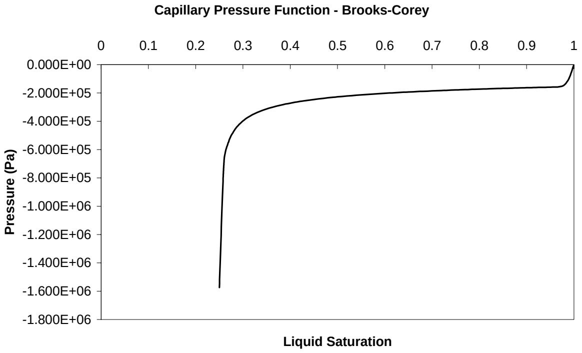

Figure 3: Capillary pressure function for the upper part of Class 1W reservoir (Brooks-Corey)

Governing mass and energy balance equations and their simultaneous solution are discussed in detail else where (Moridis at al, 2005 & Moridis, 2002).

Simplifying Assumptions

The only 2 mass components considered are water and methane. However, there are 4 phases: hydrate, ice, aqueous, gas.

Hydrate number (N_H) is considered to be constant and equal to 6. Then, hydrate is formed according to equation:

$$CH_{4(gas)} + 6.H_2O_{(liq)} \leftrightarrow CH_4.6.H_2O_{(solid)}$$

Hydrate thermal conductivity, specific heat and density are all considered to be constants and their values are presented in Table 1.

Table 1: ***Hydrate Properties***

Density	920 kg/m3
Specific Heat	2100 J/kg °C
Heat Conductivity	0.45 W/m °C

RESERVOIR MODEL

The cylindrical volumetric reservoir (Figure 4), which has a single well at the center and is modeled using radial grids, has been studied previously by Moridis et al. (1998) to compare with the earlier study of Holder et al. (1982)

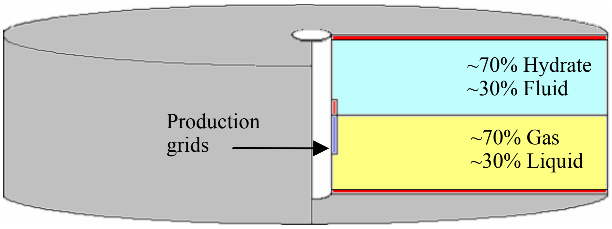

Figure 4: Schematic of the theoretical reservoir (not to scale)

Reservoir is 30 meters thick and has a radius of 567.5 meters. In addition, 1.001 meter thick intervals are added to the top and bottom of the reservoir to provide the necessary boundary conditions. Hence, height of the grid structure has been extended to 32.002 meters.

Reservoir rock is assumed to be sandstone with uniform porosity (30%) and permeability (44 md). Reservoir rock properties are given in Table 2 (Moridis et al., 1998).

Table 2: Reservoir rock properties

Density	2600 kg/m^3
Porosity	30%
Permeability	4.3425*10^{-14} m^2 (~44 md)
Specific heat	1000 J/kg ^{o}C
Heat conductivity (wet)	3.1 W/m ^{o}C
Heat conductivity (dry)	0.5 W/m ^{o}C
Pore compressibility	1.0*10^{-8} Pa^{-1}

Grid Structure

For Class 1G reservoir grid structure is composed of 77 radial elements in each one of the 48 layers, which makes a total of 3696 grids. In every layer, the radial distance between the first 4 consecutive grids is same and 0.5 meters. Then there are 73 grids with logarithmically increasing distance between them (Figure 5).

For Class 1W reservoir, grid structure was slightly different. It is composed of 99 radial elements with 48 layers in vertical direction, which makes a total of 4752 grids. In all layers, the radial distance between the first two grids is 0.1 meter, and then 5 consecutive grids are the same with 0.2 meters. Afterwards, there are 93 grids with logarithmically increasing distance between them.

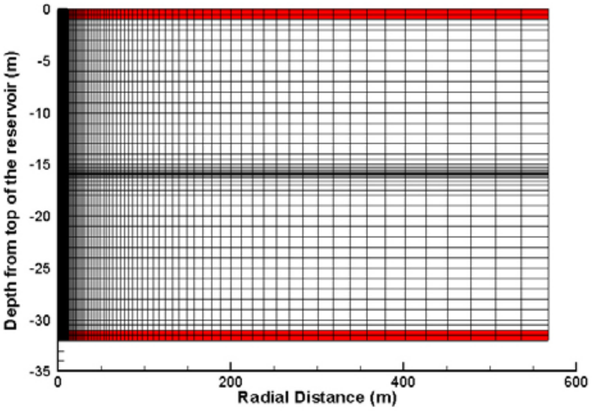

Figure 5: Grid structure of whole reservoir

To model impermeable and constant temperature boundary conditions, both at the top and bottom of reservoir 3 layer intervals were defined. The outermost layers at the top and bottom are very thin and are assigned the constant boundary temperatures. The following 2 layers are of 0.5 meters thick with no permeability and/or porosity and added solely for better description of heat flux to the actual reservoir.

Model Initialization

The most important aspect of model initialization is to obtain the same heat flux from the upper and lower parts of the dissociation front. This is needed in order to keep the position of front stable. The detailed procedure for obtaining equal heat flux from both parts is given by Moridis et.al (2005).

When high saturation and high thermal conductivity of hydrate in the upper part is considered, it is obvious that a temperature value higher than the geothermal gradient should be assigned for the sake of obtaining steady-state initial conditions with a stable dissociation front (Figure 6 & Figure 7).

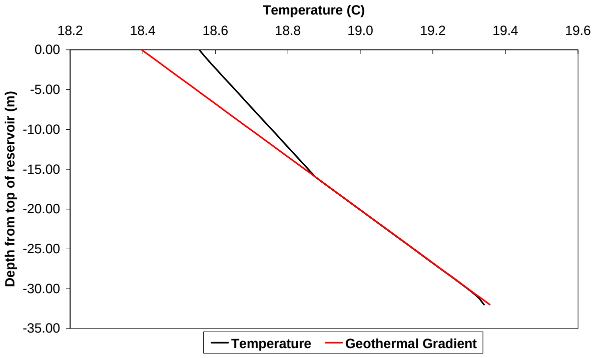

Figure 6: Initial vertical temperature distribution for Class 1G.

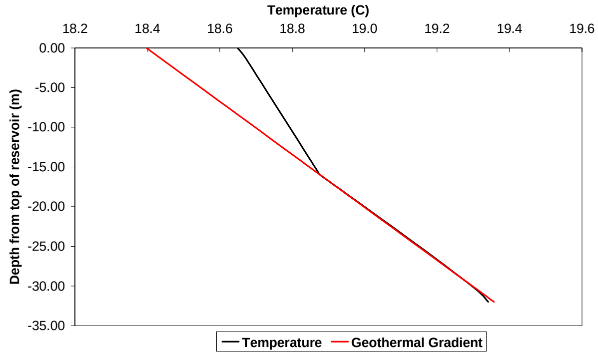

Figure 7: Initial vertical temperature distribution for Class 1W.

The proposed initial condition for the hypothetical reservoir is a pressure of 20,684,250 Pa (~3000 psi) and a corresponding equilibrium (hydrate formation) temperature of 18.8757 °C at the dissociation front that is found practically in the middle of reservoir. Upper half of the reservoir (top 15 meters) has 70% hydrate saturation while the lower half of the reservoir has a free gas saturation of 70% and 30% of liquid water, initially. Figure 8 shows the vertical temperature and pressure distribution along the reservoir as reference to hydrate equilibrium curve for pure methane.

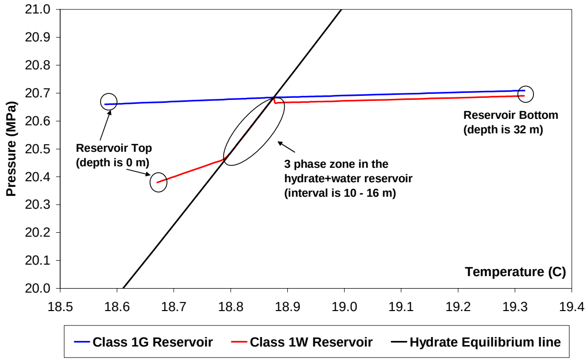

Figure 8: Initial Pressure-Temperature diagrams of Class 1G & Class 1W.

Initial saturation distributions obtained after the establishment of steady-state in the reservoir are shown in Figure 9a, Figure 11a & Figure 13a.

PRODUCTION MODELING

Because upper half of the reservoir is mostly occupied by solid hydrate, thus will not be significantly contributing to flow initially, it is presumed that well is completed in the top 10 meters of lower free gas zone and in each case study a constant mass production rate of 0.555 kg/s (1137 MMCF/day equivalent) is specified. This constant mass production rate is rationed (according to grid volume) to the 1st column of small grids in the immediate vicinity of well bore (which are indeed the innermost grids and top 10 meters of free gas zone, 16.101-26.001 meters). TOUGH-Fx computes how much of which phase is produced in a grid from the phase mobility prevailing at that grid.

Production modeling is studied both with heat addition along the well bore (case A) and without any heat addition (case B). In case A, again to the 1st column of small grids in the immediate vicinity of well bore (15.251-26.001 m), 200 W/m heat is added during whole production period.

RESULTS & DISCUSSION

Though a production period of 30 years was intended, it was not possible to obtain the data in all the cases. For instance; in case B of Class 1W, the simulation stopped very early at 0.8 year. This was due to high amount of hydrate formation in and near producing grids. The hydrate saturation was so high that it did not allow any fluid flow into or out of the grids, so the well, hence the simulation was shut down.

Hydrate Saturation Distributions

When hydrate saturation distributions for the studied cases are considered (Figure 10, Figure 11, Figure 12 & Figure 13), it is apparent that 2 distinct dissociation patterns arise for the Class 1G and 1W.

For Class 1G reservoir, analysis of Figure 9, Figure 11 and Figure 13 indicate that there is a large portion of hydrate decomposing at the top of the hydrate zone, in addition to dissociation front (both for case A and case B). This is attributed to the fact that the whole hydrate zone cools while supplying heat to the dissociation front. Though a pressure drop is observed in the hydrate zone due to production (Figure 15), because of the cooling zone remained at the hydrate equilibrium conditions initially. As the zone gets colder, a decreasing temperature gradient develops along the hydrate zone, while the top constant temperature boundary is always supplying heat to the system. Then, it was just a matter of time before suitable P-T conditions established and hydrate zone began to decompose from the top as well.

Hydrate saturation change in the first 10 m radial distance shows a structure resembling flow channels with low hydrate saturations, which is valid for both cases A & B (Figure 11c & d, Figure 13c & d). These pseudo flow channels are slanted as if coinciding with streamlines of flow. While hydrate saturation decreases along the channels, high saturation is observed along the inclined bands that separate the channels. Grids of the bands supply the heat needed for decomposition to the neighboring flow channel grids thus their own hydrate content grow higher with draining water and limits their contribution to the flow. This is why higher pressures are observed in these cells.

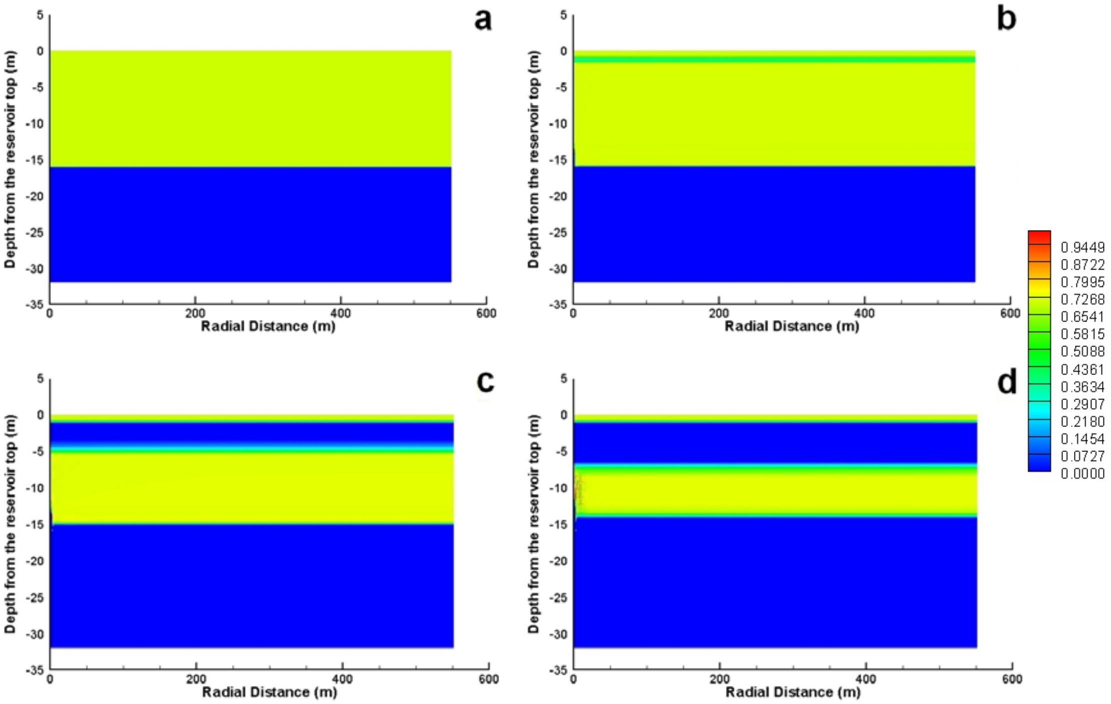

Figure 9: Hydrate saturation distribution (fraction) for whole reservoir, Class 1G – heating (a = 1.5 days, b = 5 years, c = 20 years and d = 30 years)

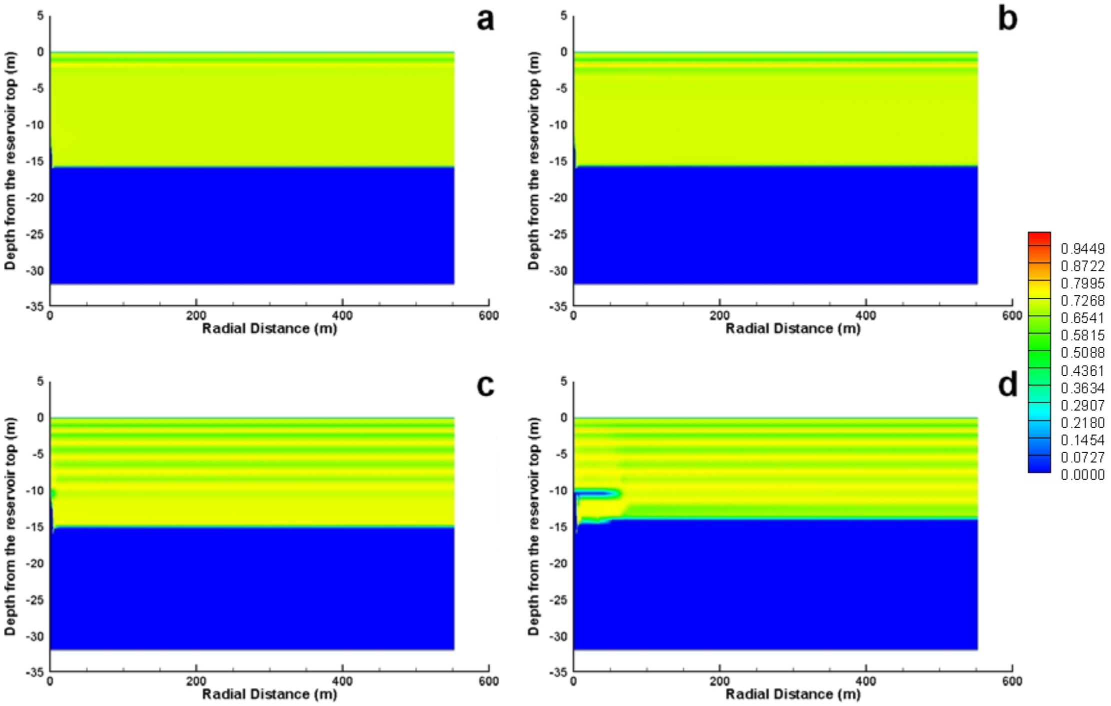

Figure 10: Hydrate saturation distribution (fraction) for whole reservoir, Class 1W – heating (a = 4 years, b = 5 years, c = 10 years and d = 15 years)

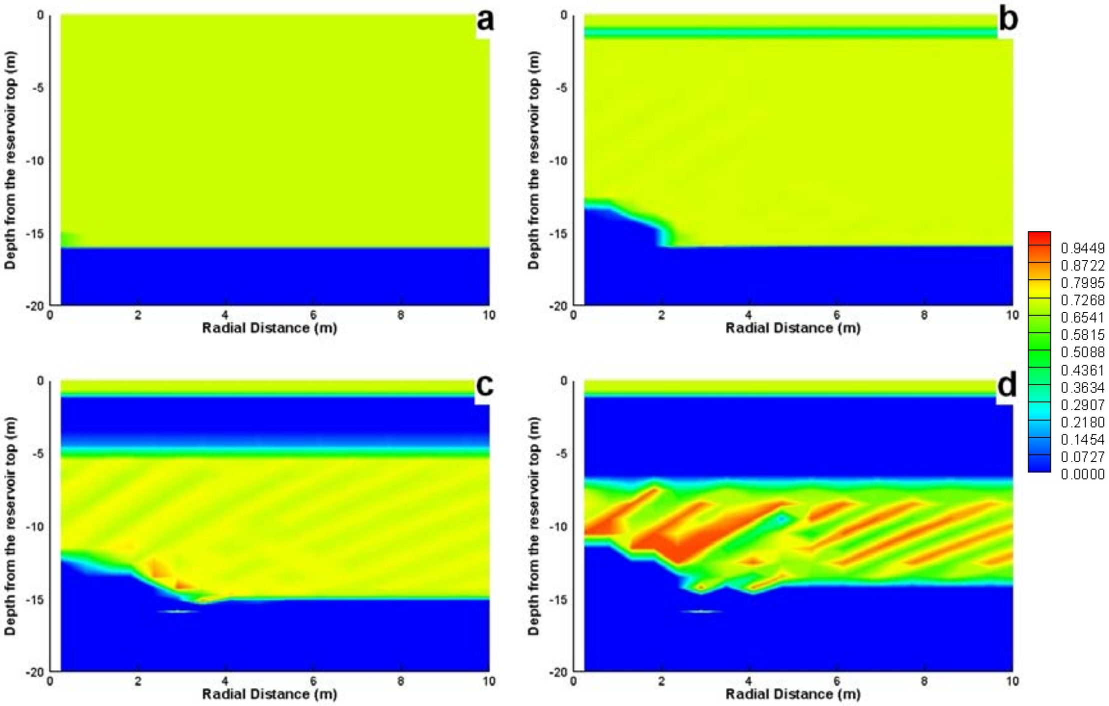

Figure 11: Hydrate saturation distribution (fraction) near well-bore, Class 1G – heating (a = 1.5 days, b = 5 years, c = 20 years and d = 30 years)

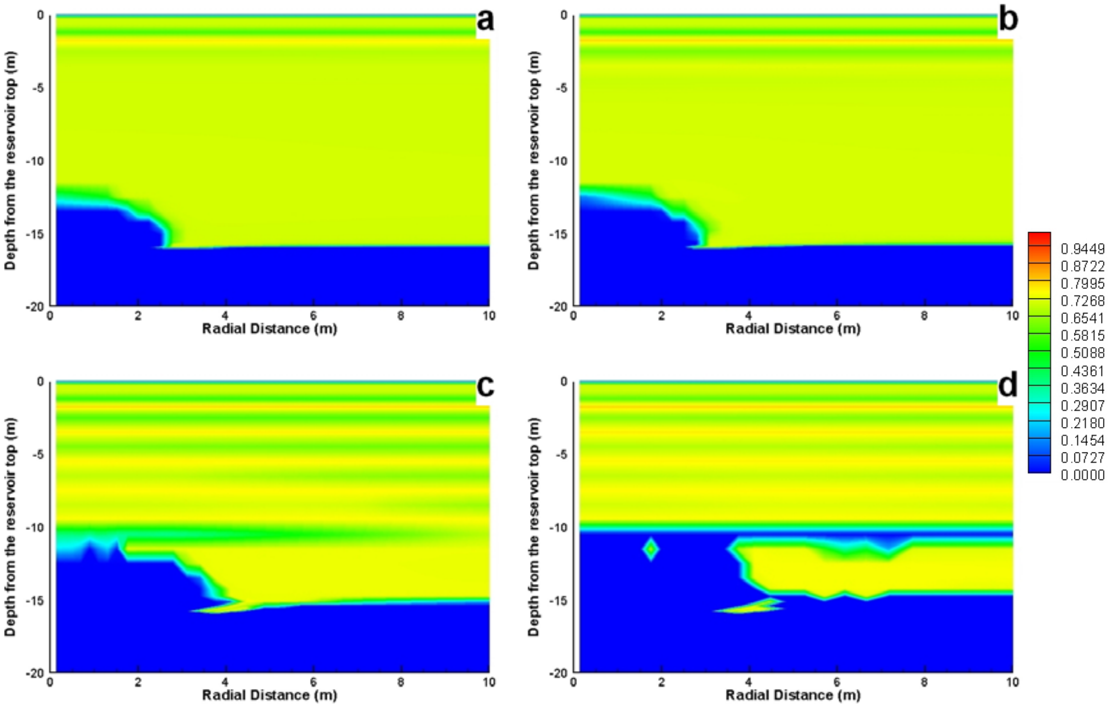

Figure 12: Hydrate saturation distribution (fraction) near well-bore, Class 1W – heating (a = 4 years, b = 5 years, c = 10 years and d = 15 years)

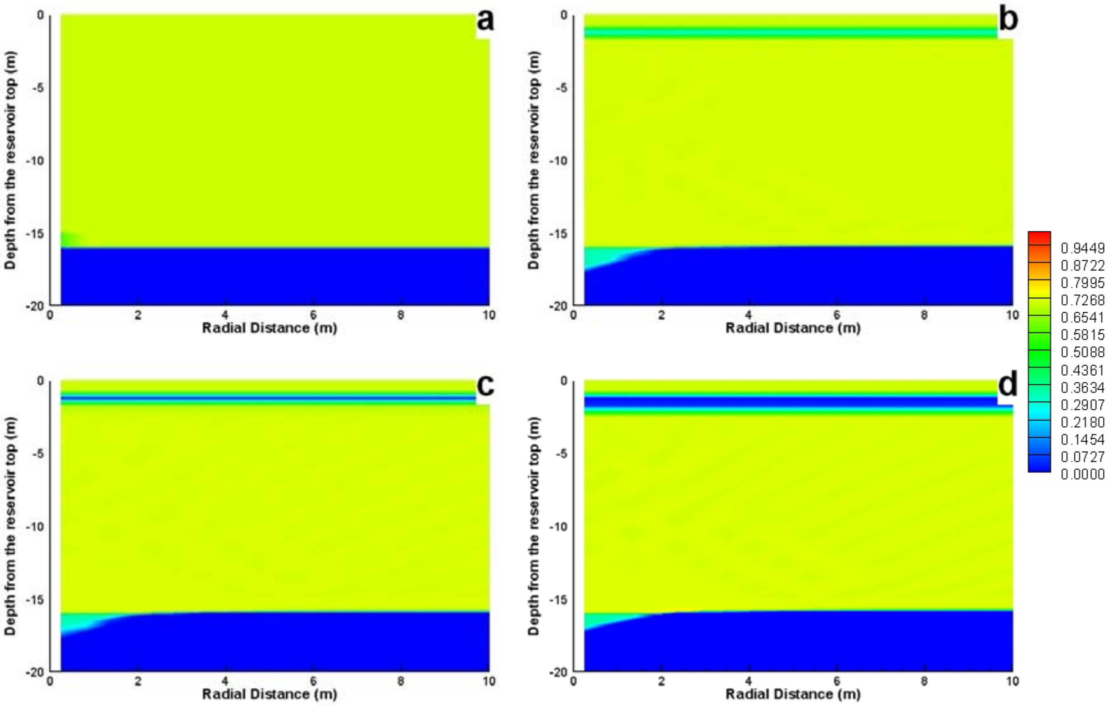

Figure 13: Hydrate saturation distribution (fraction) near well-bore, Class 1G – no heating (a = 1 day, b = 5 years, c = 6 years and d = 8 years)

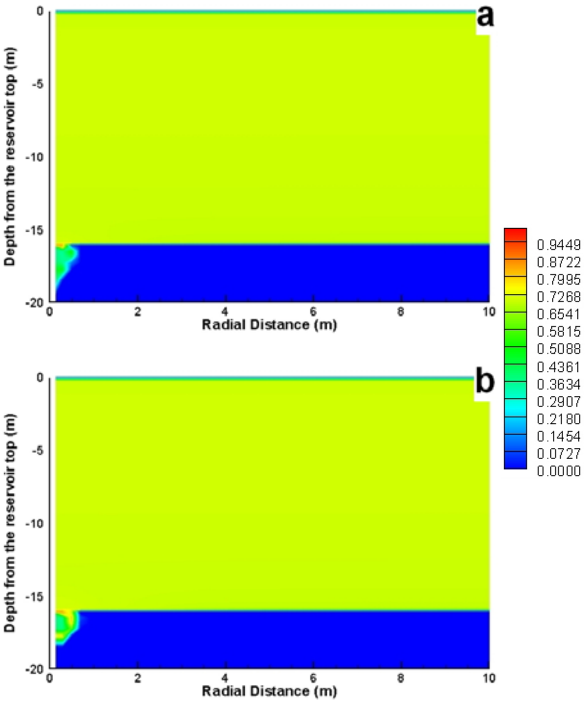

Figure 14: Hydrate saturation distribution (fraction) near well-bore, Class 1W – no heating (a = 6 months, b = 9 months)

In Figure 15, hydrate equilibrium pressure line (which is an indicator of system temperature) is initially below the system pressure in the hydrate zone. At about 5 years of production, pressure profile in the hydrate zone coincides with the hydrate equilibrium pressure indicating that the whole hydrate zone is in dissociation stage. After 10 years of production, system pressure is less than hydrate equilibrium pressure. Yet, the region experiencing the greatest pressure drop and where decomposed gas can freely flow is the original dissociation front. Therefore, hydrate zone cools not only because of the dissociation occurring all over the zone, but also these decomposing layers are supplying heat to the front where temperature decrease is more (due to dissociation). Then, first the top layer begins to decompose due to heat from the constant temperature boundary found just above. Hence another dissociation front is created at the top. This second front shows similar characteristics to the actual front.

For Class 1W reservoir, analysis of Figure 10 & Figure 12 indicate that with 4th year of production, formations which resemble an inverse ice lens structure began to appear at the top of hydrate zone. The reason of such successive, low-high alternating hydrate saturation bands can be deduced from the pressure profiles for Class 1W (Figure 16).

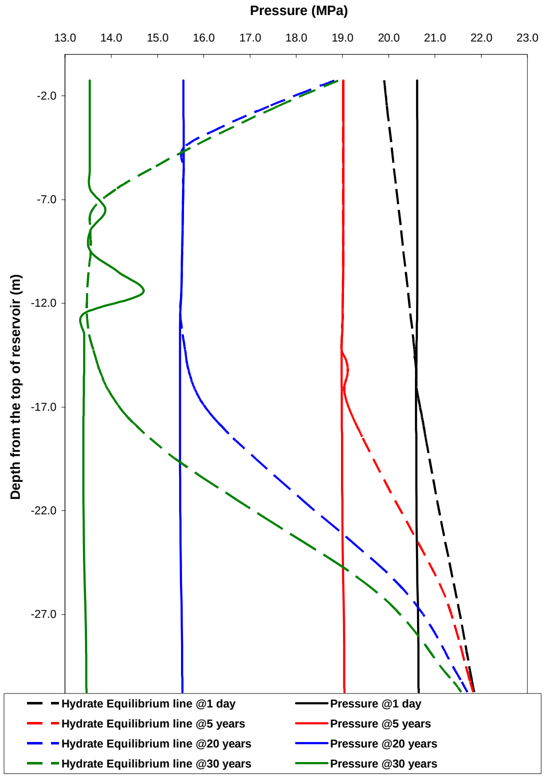

Figure 15: Pressure profile for Class 1G – heating

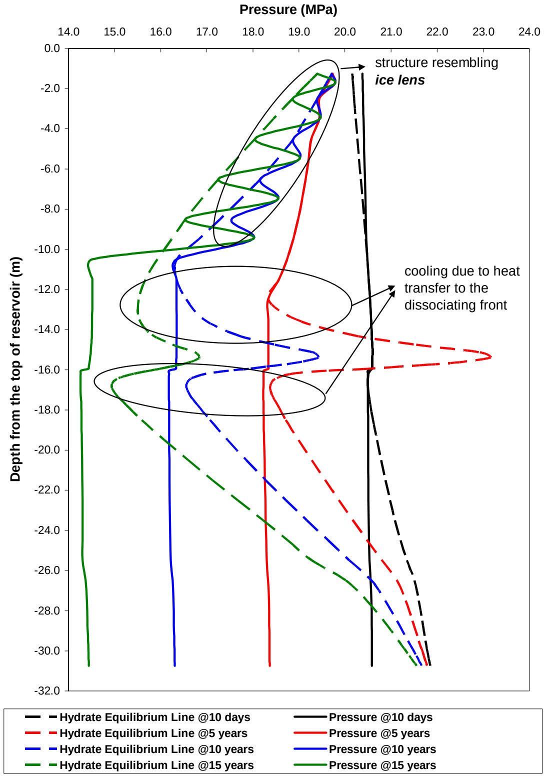

Figure 16: Pressure profile for Class 1W – heating

Initially, in Figure 16, hydrate equilibrium line is below the system pressure in the hydrate zone. Later, decreasing pressure (because of production) and temperature gradients (due to decomposition) develop in the hydrate zone. Starting with year 3, system pressure meets hydrate equilibrium line and decomposition is initiated in the top layers of hydrate zone. When the text output of the simulation is examined for these layers, it is seen that at 3rd year 2 of the upper most layers (interval 1-2 meters) are both decomposing. After a very short while (at 3.5 years), only the top layer continues to decompose as opposed to the layer just below it where hydrate saturation begins to increase (at equilibrium conditions). Increasing hydrate saturation seals the 2nd layer and decreases the flow from these 2 layers (year 5). There is built a no flow boundary acting only as a heat conducting strata because water saturation decreased below irreducible with increasing hydrate amount. So, a similar horizontal low-high hydrate saturation structure begins to develop in the following 2 layers and this chain of low-high saturation bands extent to the dissociation front during the rest of the production.

Then it is possible to conclude that the reason why two different hydrate saturation patterns occur in the different class of hydrate reservoirs is because of very high capillary pressure acting on the liquid phase in Class 1W. In Class 1G, gas and released water can easily flow towards producing grids without being impeded by high capillary pressure keeping water stagnant. Yet, in Class 1W, water remained in the grids due to high capillary pressure and this further prevented released gas from easily flowing (by reducing relative permeability to it). When released water and gas could not be moved from their initial locations, they caused an increase in the pressure and thus re-formation of hydrate.

In Class 1W, around year 9 (Figure 12c), the low saturation hydrate layer at 10 meter depth begun to decompose all of the its hydrate because the cavity in hydrate zone near the well-bore has grown so large that there established a gap of no hydrate grids where liberated gas in the layer at 10 meter could easily flow through to the producing elements.

Effect of Well-bore Heating

Effect of well-bore heating is very obvious when hydrate saturation distributions of case A and case B, of both reservoir types are compared (Figure 11, Figure 12, Figure 13 & Figure 14). Formation of hydrate at and near the producing grids is clear. Also, it is understood that in case A, the cavity forming near the well-bore due to dissolution of hydrate should be solely due to this heating.

One important point here is, in case B of Class 1G (Figure 13) the saturation of newly formed hydrate around the production grids is low enough to permit a continuous flow, thus it was possible to obtain more than 8 years long production with out heating. Moreover, for Class 1G, because in case B some of the water is captured in the hydrate near and at the producing elements and permeability to water has decreased due to solid saturation, amount of produced water is less than case A.

On the other hand, in case B of Class 1W (Figure 14) the amount of new hydrate formation near the producing grids is too high and restricts the flow. The reason of hydrate formation at high saturations is the existence of enough water and gas to form hydrate. Eventually, the simulation is shut-down when fluids can no longer be supplied to producing elements at the specified rates.

Apparently, the rate of production and depth of completion (location of production) determines whether well-bore heating is required for the depressurization scheme. Producing elements had better be placed as far as possible from the dissociation front.

Replenishment of Produced Methane

Replenishment is the contribution of released methane to the free gas in the reservoir. This means how much of the produced free methane was restored back into the reservoir through dissolution of hydrate. From Figure 17, it is apparent that replenishment in cases A and B are the same (during the first 8 years of production) for Class 1G; suggesting that the low saturation of hydrate formed around the production grids in Case B did not choke the gas production.

For Class 1G, the great take off in the replenishment plot of cases A and B after 2nd year of production is evidently attributed to development of the second dissociation front at the top of hydrate zone.

The large rate decrease at years 6, 8, 12 & 16.5 in the replenishment graphs of cases A and B of Class 1G are due to complete depletion of hydrates in the layer where the second (upper) dissociating front is. This is because the layer below the second front is initially colder and it takes sometime before decomposition could be re-initiated in this new layer of dissociation front. Following continuous rise in the graph during a long period of time shows how decomposition rate increases with decreasing hydrate in the layer. It is obvious from Figure 17 that the replenishment rate of methane production is as high as ~50% for Case A in 20 years production life. On the other hand, the cumulative replenishment of produced methane from hydrate reaches to ~38% (Figure 18).

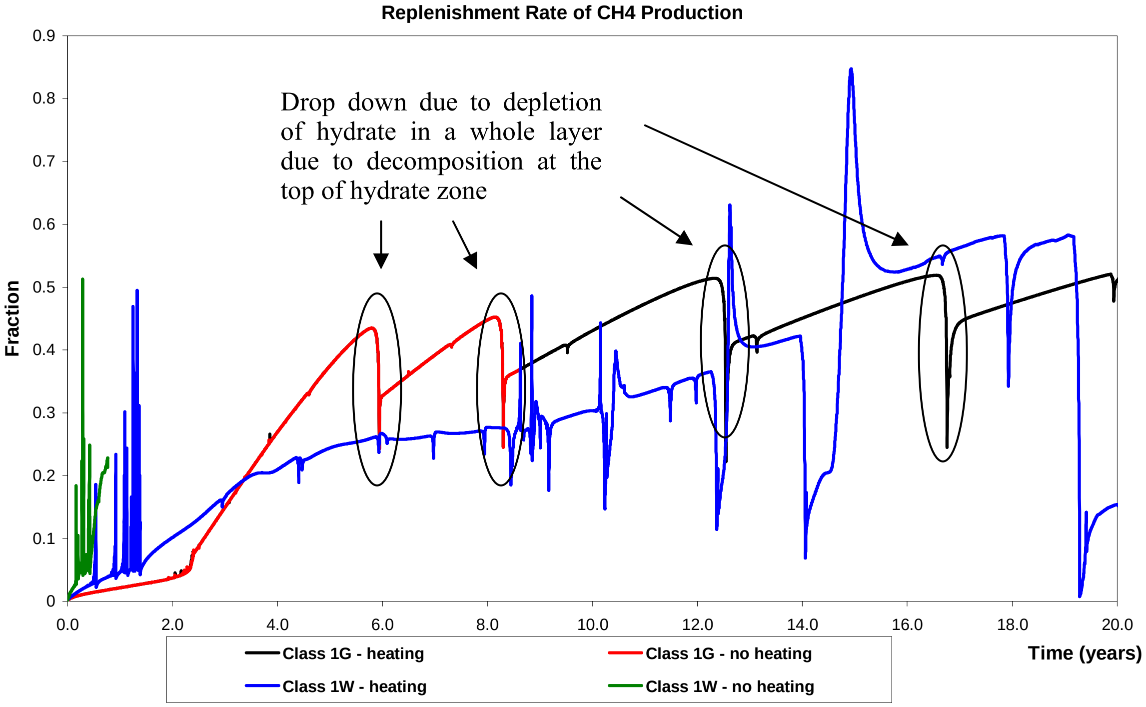

Figure 17: Production replenishment rate, fraction (or methane release rate)

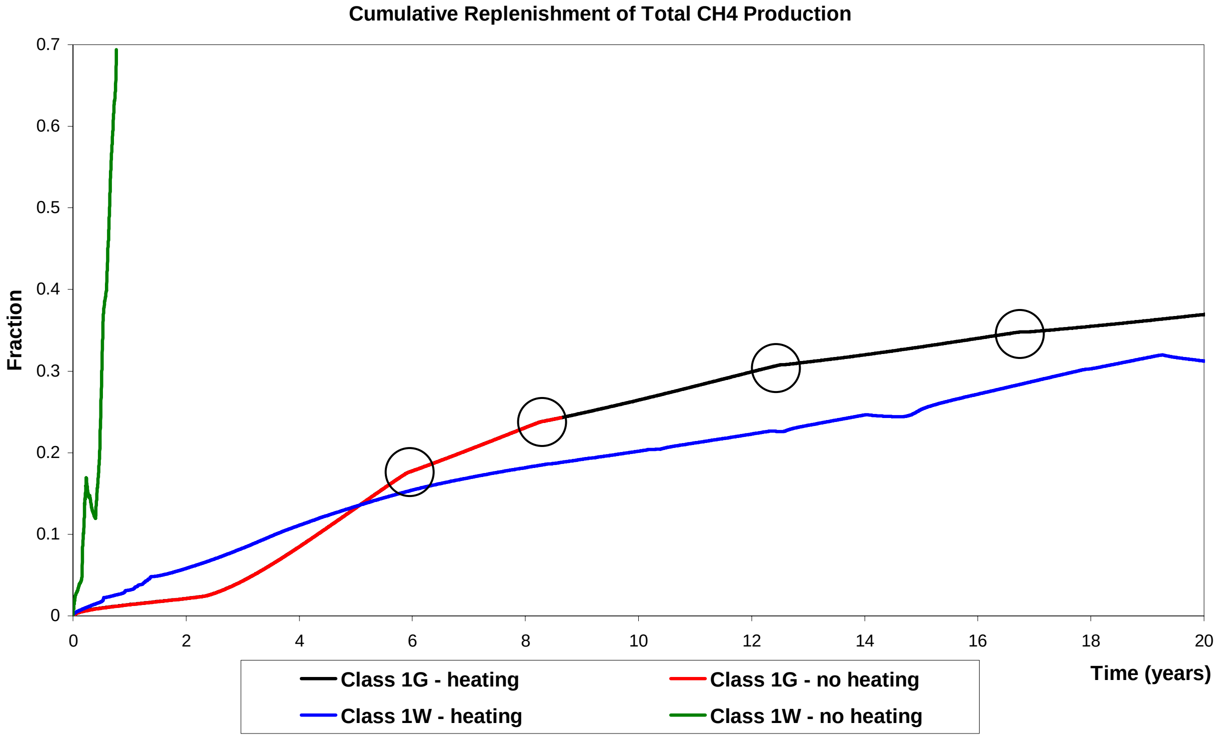

Figure 18: Cumulative production replenishment, fraction (or total methane released)

For Class 1W, acute increases in methane release rate observed in case A & B (Figure 17, 1st 2 year period) are attributed to the fact that, because compressibility of water is quite low compared to gases, the pressure drop due to production is sensed in the whole hydrate zone and therefore decomposition is induced in all of the upper hydrate section.

Similar to Class 1G, the drops in methane release, which is a result of wiping out of hydrate in the layer of original dissociation front, are quickly restored by the initiation of decomposition in the new layer of front.

Compared to case A of Class 1W, it takes a longer period to reestablish the rapid rate of decomposition in Class 1G. This is because gas released from the second (upper) front can expand only to the space left by previously emptied layer and released water has to move down. But in case A of Class 1W, because the main contribution is from the primary (original) front and released water and gas can expand more freely, the rate is quickly restored.

Effect of Different Capillary Pressure Function

The modified Brooks-Corey capillary pressure function used in this study is a function of liquid saturation alone. Hence, it would not let the water drain from the upper section unless its saturation is above 90% (Figure 3). The most obvious implication of this is the built up of a liquid barrier in the middle of reservoir (Figure 19), hindering released gas & water flow (Moridis et al., 2005). This in turn means that results obtained for Class 1W are tentative and represent a worst case scenario because gas withdrawal is hindered by this barrier. Also; as can be seen in Figure 16, hydrate equilibrium line (dashed lines) develops a sharp front towards the location of this barrier since decomposed warm water accumulates here.

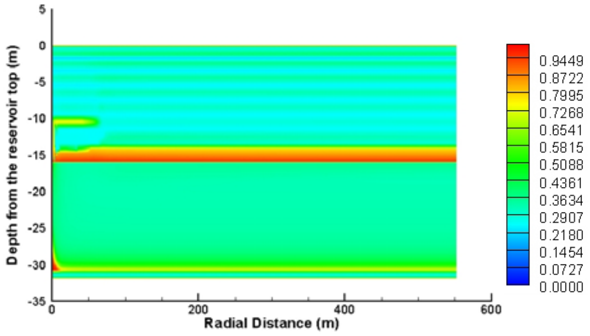

Figure 19: Water saturation distribution (fraction) for whole reservoir, Class 1W – heating (15 years)

Comparison with Previous Work

In the articles of Holder et al., (1982) and Moridis (2002), cumulative methane replenishment within the first 3 years of production is as high as 21% and 72% respectively and it is not mentioned in the texts whether any ice lens formation or secondary dissociation front at the top of hydrate zone is observed.

In this study, cumulative contribution of released gas for the first 3 years has been around 10% (Figure 18, Class 1W, case A), significantly lower than previous studies and this is attributed mainly to the fact that a very strong capillary pressure has been assigned in the upper section of reservoir causing the least release from hydrates by preventing water from draining (actually, Holder et al., 1982, assumed a linear, smoothed dissociation front acting as a moving boundary of impermeable hydrate zone).

CONCLUSIONS

The results of this study indicate that:

- For Class 1G reservoirs, a second dissociation front develops at the top of hydrate zone and has the most substantial contribution to replenishment.
- For Class 1G reservoirs, near the well-bore, slanted pseudo flow channels develop coinciding with the streamlines of flow.
- For Class 1W reservoirs, because the second dissociation front could not fully develop due to high capillary pressure acting on liquid phase, high-low hydrate saturation bands (a structure similar to the inverse of ice lens formation) is observed.
- Near well-bore cavity in hydrate saturation occurs only when well-bore heating is applied and well-bore heating may not be necessary if production is not close to the primary dissociation front.
- Rate of replenishment of gas production is up to ~50% for both types of hydrate deposition and replenishment of total methane volume is up to ~38% for Class 1G and up to ~30% for Class 1W for 20 years production life.
- Initial cumulative replenishment (first 3.5 years in Figure 17) and the replenishment rate (first 5 years in Figure 18) are higher for Class 1W because the pressure drop induced by production is immediately felt all over the reservoir due to low compressibility of water.
- When Class 1W results are compared to the previous works of Holder et al. (1982) and Moridis (2002), amount of released gas contribution within the first 3 years of production is significantly low which is primarily attributed to the specified high capillary pressure function.
- Because a second dissociation front develops at the top of hydrate zone, this region should as well be modeled using finer (thinner) layers.
- The effect of the number and thickness of no porosity boundary layers, which are provided at the top and bottom of reservoir in order to describe heat flux from surrounding strata, should be further investigated to see their effect on the development of second dissociation front as well as the hydrate lens sequence.
- Not only permeability but also capillary pressure should be defined as a function of solid saturation.

ACKNOWLEDGMENT

The LBNL component of this study was supported by the Assistant Secretary for Fossil Energy, Office of Natural Gas and Petroleum Technology, through the National Energy Technology Laboratory, under the U.S. Department of Energy, Contract No. DE-AC03-76SF00098.

REFERENCES

Moridis, G.J. and Collet T.S., *Gas Production from Class 1 Hydrate Accumulations*, Report LBNL-52827, Lawrence Berkeley National Laboratory, Berkeley, Calif., 2003.

Moridis, G.J. Kowalsky, M.B. and Pruess, K, *TOUGH-Fx/HYDRATE v1.0 User's Manual: A Code for the Simulation of System Behavior in Hydrate Bearing Geologic Media*, LBNL, 2005.

Pruess, K., C. Oldenburg, and G. Moridis, *TOUGH2 User's Guide, Version 2.0*, Report LBNL-43134, Lawrence Berkeley National Laboratory, Berkeley, Calif., 1999.

Moridis, G.J, Numerical Studies of Gas Production from Methane Hydrates, SPE 75691, 2002.

Sloan, E.D. Jr., *Clathrate Hydrates of Natural Gases*, Marcel Dekker, NY, 641 pp. 1990.

Moridis, G.J., Apps, J., Pruess, K., and Myer, L., *EOSHYDR: A TOUGH2 Module for CH4 – Hydrate Release and Flow in the Subsurface*, Report LBNL-42386, 1998.

Holder, G.D. and Angert, P.F., Simulation of Gas Production from a Reservoir Containing Both Gas Hydrates and Free Natural Gas, SPE 11105, 1982.

Moridis, G.J, Numerical Studies of Gas Production from Methane Hydrates, SPE 75691, 2002.

Moridis, G.J. Kowalsky, M.B. and Pruess, K, Depressurization-Induced Gas Production from Class 1 Hydrate Deposits, SPE 97266, 2005.

Alp, D., *Gas Production from Hydrate Reservoirs*, M.Sc. Thesis, Middle East Technical University, 149 pp., 2005.

NOMENCLATURE

ΔH , dissociation enthalpy, J

k_0 is the absolute permeability

k_β is the effective permeability to phase β

$k_{r\beta}$ is the relative permeability to phase β

k_{dry} is thermal conductivity of dry rock

k_{wet} is thermal conductivity of wet rock

P is system pressure, Pa

Pe is equilibrium pressure in MPa

R, gas constant 8.316, J/mole/K

S_A is aqueous phase saturation

S_H is hydrate saturation

S_I is ice saturation

S_{lr} and $S_{lr}^{'}$ are irreducible liquid saturation

S_{gr} is irreducible gas saturation

T is system temperature, K

z, gas compressibility factor

λ_I is thermal conductivity of ice